Biochemical Pharmacology 242 (2025) 117398

Contents lists available at ScienceDirect

Biochemical Pharmacology

journal homepage: www.elsevier.com/locate/biochempharm

Dual targeting of EphAs and KDR axis hampers VEGF-induced angiogenesis and glioma stem cell replication

Alfonso Zappia [a,1], Francesca Romana Ferrari [a,1], Carmine Giorgio [a], Stefano Sala [a], Ilaria Zanotti [a], Simona Parrinello [b], Melanie P. Clements [b], Marco Rusnati [c,d], Michela Corsini [c], Andrea Blesio [a], Riccardo Castelli [a], Lorenzo Guidetti [a], Laura Scalvini [a], Alessio Lodola [a,*], Massimiliano Tognolini [a,*]

[a] Dipartimento di Scienze degli Alimenti e del Farmaco, Università degli studi di Parma, Parco Area delle Scienze 27/A, 43124 Parma, Italy
[b] Samantha Dickson Brain Cancer Unit, UCL Cancer Institute, London WC1E 6DD, UK
[c] Department of Molecular and Translational Medicine, University of Brescia 25123 Brescia, Italy
[d] Consorzio Interuniversitario Biotecnologie (CIB), Unit of Brescia, Brescia, Italy

A B S T R A C T

Glioblastoma multiforme (GBM) is an aggressive and highly vascularized brain tumor with a poor prognosis and limited therapeutic options. Resistance to current treatments is largely driven by glioma stem-like cells (GSCs), a subpopulation with high tumorigenic potential that plays a key role in tumor progression, recurrence, and angiogenesis.

Eph receptor tyrosine kinases, including EphA and EphB, are broadly implicated in GBM biology. While both classes contribute to tumor development and plasticity, EphA receptors are more directly involved in GSC maintenance and in crosstalk with the VEGF/VEGFR-2 axis, whereas EphB receptor dysregulation may promote tumor invasion. This subclass distinction makes selective targeting of EphA receptors an attractive therapeutic strategy.

Here, we present the characterization of UniPR1449, a novel selective EphA receptor inhibitor. UniPR1449 is a protein–protein interaction inhibitor (PPI-i) that blocks ephrin-A1-induced EphA2 phosphorylation, internalization, and degradation in GBM cell lines. In patient-derived GSCs, the compound significantly reduces proliferation and S-phase entry. Additionally, UniPR1449 impairs VEGF-induced angiogenesis in the chick chorioallantoic membrane (CAM) assay, while leaving FGF2-mediated vascularization unaffected.

This dual mechanism of action—targeting both EphA signaling and VEGFR-2-mediated angiogenesis—highlights its therapeutic potential in addressing two key pathological features of GBM: vascular support and stem-like tumor cell renewal. Moreover, the selectivity displayed by UniPR1449 for EphA receptors may offer a safety advantage over pan-Eph inhibitors, which could disrupt physiological EphB functions.

Together, these results position UniPR1449 as a promising lead compound for the development of multitarget therapies against GBM.

1. Introduction

Eph receptors, the largest family of tyrosine kinase receptors in mammals, were initially identified in erythropoietin-producing hepatocellular carcinoma cells [1]. They includes EphAs (10 receptors) and EphBs (6 receptors), interacting with ephrin ligands to mediate cell–cell communication. Ephrin-As are GPI-anchored proteins, while ephrin-Bs are transmembrane proteins with an intracellular domain. Eph receptors and ephrins interact promiscuously with each other, with ephrin-As usually binding EphA receptors, and ephrin-Bs binding EphB receptors. The Eph-ephrin system enables bidirectional signaling: a "forward" signal in the Eph receptor-bearing cell and a "reverse" signal in the ephrin-expressing cell [2,3]. The Eph-ephrin system physiologically contributes to the regulation of axonal guidance, gut tissue regeneration and vasculogenesis. Compelling evidences, accumulated in more than 30 years, have demonstrated that the dysregulation of the Eph-ephrin system is linked to the onset and progression of a variety of cancer diseases [3]. The Eph-ephrin system controls the communication between cancer cells and the tumour microenvironment (TME) promoting tumour angiogenesis and vascular mimicry, a hypoxia-driven process which involves the assembly of tumour cells into blood vessel-like structures [4]. Recent findings have pointed out a clear connection between the onset of glioblastoma (GBM) and the Eph-ephrin system. High expression of EphA2 and/or EphA3 has been correlated to

* Corresponding authors.
E-mail addresses: Alessio.lodola@unipr.it (A. Lodola), Massimiliano.tognolini@unipr.it (M. Tognolini).
[1] These authors equally contributed to the work.

https://doi.org/10.1016/j.bcp.2025.117398
Received 29 May 2025; Received in revised form 26 September 2025; Accepted 3 October 2025
Available online 3 October 2025

poor survival of GBM patients [5,6], while EphB4 and ephrin-B2 have been found to contribute to proliferation and in the invasive potential of GBM [7].

Standard treatment of GBM includes tumor resection, radiotherapy, and chemiotherapy, based on the administration of the alkylating agent temozolomide (TMZ). However, GBM is characterized by poor responsiveness to classical radio- and chemotherapy and by the rapid selection of resistance clones. This resistance is partly attributed to GBM stem-like cells (GSCs), a subpopulation of self-renewing, highly tumorigenic cells associated with vascular niches [8]. Additionally, GSCs contribute to GBM heterogeneity, progression, and recurrence [9–12].

Eph receptors are directly involved in GBM onset and progression [13,14] by favouring the survival of GSCs. In particular, EphA2 is able to promote GSCs self-renewal [13,15,16], while EphA3 enhances their proliferation *via* MAPK signaling [6]. Furthermore, EphB4-ephrin-B2 modulates GSCs migration and proliferation by disrupting vascular confinement [17].

Tumor vascularization in GBM is mainly driven by the VEGF-A/VEGFR-2 (KDR) axis, together with other molecular partners including integrins, neuropilin, and the Eph-ephrin system itself. EphA2 regulates VEGFR-2 expression in GBM cells and controls vessel sprouting *via* VEGFR-2, independently of VEGF [18]. Taken together, this evidence points out the molecular targeting of the Eph/ephrin system as a promising cancer therapeutic strategy in GBM [19].

The research of our laboratories has been focusing on the preclinical development of Eph-ephrin interaction inhibitors for years [20]. Our efforts culminated in the discovery of UniPR1331, a pan Eph-ephrin antagonist with significant antiangiogenic and antivasculogenic properties, which blocks the growth of GBM tumor in both xenograft and orthotopic mice models [21]. The anti GBM activity of this compound has been linked to its ability to reduce the self-renewing and the multipotent differentiation potential of GSCs, two phenomena that impair vasculomimicry. A follow-up investigation on UniPR1331 has shown that this compound is also able to block VEGFR-mediated angiogenesis not only through the direct inhibition of the Eph-ephrin interaction but also hampering the formation of the VEGF-VEGFR2 complex [21–23].

In this scenario, we recently described a new class of 1-(phenylsulfonyl)-1H-indole derivatives that selectively targets the EphA receptors thus sparying the EphB receptor subtypes [24,25]. In light of the peculiar biochemical profile of this new class of agents, we set to characterize the molecular mechanism of action of one of these new compounds, namely *N*-(3β-hydroxy-Δ^5-cholen-24-oyl)-1-benzensulfonyl-L-β-homotryptophan (UniPR1449, Table 1) on EphA2 activation, internalization and degradation on GBM cell lines. Furthermore, we investigated whether UniPR1449 possesses an improved potency or efficacy, in blocking proliferation of GSCs as well as in hampering angiogenenetic processes compared to the reference compound UniPR1331. To this end, UniPR1449 was tested in vitro in several cellular assays using GSCs to evaluate its direct anti GBM potential, and in a validated model of in vivo angiogenesis (i.e., the chicken chorioallantoic membrane, CAM), to evaluate its ability to prevent the formation of an ordered vascular system in the presence of growth factors, mimicking the tumor microenvironment.

Table 1
Potency of UniPR1449 on various Eph receptors [25]

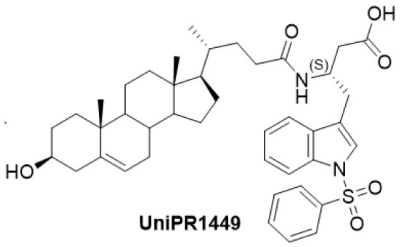

UniPR1449

	IC_{50} value (μM) (95 % CL)
EphA1	11 (4.1–28)
EphA2	8.8 (5.5–12)
EphA3	11 (5.3–22)
EphA4	6.3 (3.6–11)
EphA5	10 (6.9–15)
EphA6	11 (7.1–16)
EphA7	22 (10–50)
EphA8	5.5 (2.6–11)
EphB1	>30
EphB2	>30
EphB3	>30

2. Material and methods

2.1. Reagents

Unless otherwise specified, all culture media and supplements were bought from Euroclone (Milan, Italy), recombinant proteins and antibodies were from R&D System (Minneapolis, MN, USA), leupeptin, aprotinin, NP40, tween20, bovine serum albumin (BSA), and salts for solutions were from ITW Reagents (Chicago, IL, USA), EDTA and sodium orthovanadate were from Merck (Darmstadt, Germany). VEGFA165 (here referred to as VEGF) was provided by K. Ballmer-Hofer (PSI, Villigen, Switzerland), Dasatinib was from LC laboratories (Woburn, MA, USA). UniPR1449 (*N*-(3b-hydroxy-D^5-cholen-24-oyl)-1-benzensulfonyl-L-β-homotryptophan) was synthetized according to the previously described procedure [24]. The purity of the compound was higher than 95 %.

2.2. Cell cultures

U251 (human GBM cells) is a standard cell line naturally overexpressing EphA2 receptor [26]. They were cultured in MEM supplemented with 10 % fetal calf serum (FCS), 1 % non-essential amino acids (NEAA), 1 % sodium pyruvate, 1 % glutamine and 1 % antibiotic solution. The cell line was maintained in an incubator with a humidified atmosphere consisting of 95 % air and 5 % CO_2 at a temperature of 37 °C.

GCGR L11 Patient-derived GCGR cell line was provided by the glioma cellular genetics resource (https://www.gcgr.org.uk). It was cultured adherently in serum-free GSC media DMEM/F-12 (Thermo Fisher Scientific, Waltham, MA, USA), N2 (1/200) (Thermo Fisher Scientific, Waltham, MA, USA), B27 (1/100) (Thermo Fisher Scientific, Waltham, MA, USA), 1 mg/mL laminin (Sigma Aldrich, St. Louis, MO, USA), 10 ng/mL EGF and FGF-2 (Thermo Fisher Scientific, Waltham, MA, USA), 100x MEM NEAA (Thermo Fisher Scientific, Waltham, MA, USA), 0.1 mM 2-mercaptoethanol, 0.012 % BSA (Thermo Fisher Scientific, Waltham, MA, USA), 0.2 g/L glucose (Sigma Aldrich, St. Louis, MO, USA) and 1000 U/mL penicillin–streptomycin (Sigma Aldrich, St. Louis, MO, USA). Cells were dissociated using Accutase solution (Sigma Aldrich, St. Louis, MO, USA).

2.3. Lactate dehydrogenase (LDH) assay

Non-specific toxicity induced by UniPR1449 on U251 cells was assessed measuring the release of LDH into the cell culture medium after two hours of incubation with the compound. The cytotoxicity was evaluated using CytTox 96® nonradioactive cytotoxicity assay (Promega, Madison, WI, USA, #1780) to identify the maximal safe concentration usable in cellular functional assays. Briefly, cells were seeded in 96-well Falcon® plates (Corning, Corning, NY, USA, #353072) at a concentration of 10^5 cells/mL and the day after were serum starved. Then, cells were treated with UniPR1449 at 30, 10 μM, PBS-DMSO 0.3 % or lysis solution (10 % v/v Triton-X 100). After 2 h of incubation, the culture medium was aspirated and centrifuged at 500 g for 4 min to obtain a cell free supernatant. LDH quantification was measured using

30 min coupled enzymatic assay which results in the conversion of iodonitrotetrazolium violet (INT) into red formazan. The amount of coloration observed is proportional to the number of lysed cells and quantified at 492 nm using an ELISA Sunrise plate reader (Tecan, Männedorf, Switzerland). The results were expressed as the ratio of absorbance in treated cells compared to cells in lysis solution alone.

2.4. EphA2 phosphorylation and total EphA2

Cells were seeded in 12-well Costar® plates (Corning, Corning, NY, USA, #3513) at the concentration of 7×10^4 cells/mL, in complete medium and incubated overnight. The following day, cells were serum starved for two hours. Then, cells were treated with UniPR1449, in the presence or absence of ephrin-A1-Fc 0.1 μg/mL and vehicle or standard drug. Dasatinib, a well known kinase inhibitor, was used as positive control. At the end of the incubation, cells were rinsed with sterile PBS and solubilized in lysis buffer (1 % NP-40, 20 mM Tris (pH 8.0), 137 mM NaCl, 10 % glycerol, 2 mM EDTA, 1 mM activated sodium orthovanadate, 10 μg/mL aprotinin, and 10 μg/mL leupeptin). The lysates were resuspended and rocked at 4° C for 30 min and then centrifugated at 2000 g for 5 min at 4 °C. The protein content of supernatant was measured with BCA protein assay kit (Thermo Fisher Scientific, Waltham, MA, USA, #23250). EphA2 phosphorylation and total EphA2 were measured in cell lysates using a DuoSet® IC Human Phospho-EphA2 ELISA Kit (R&D Systems, Minneapolis, MN, USA, #DYC4056), following the manufacturer's protocol. Briefly, 96-well ELISA high binding Costar® plate (Corning, Corning, NY, USA, #9018) was incubated overnight at room temperature with 100 μL/well of EphA2 capture antibody diluted in sterile PBS to the appropriate working concentration. After blocking, the wells were incubated for 2 h at room temperature with 100 μL/well of lysate, followed by 2 h incubation at room temperature with the detection antibody (R&D Systems, Minneapolis, MN, USA, anti-pTyr contained in #DYC4056 kit for phospho EphA2, anti-EphA2 #MAB3035 for total EphA2) diluted in sterile PBS + 0.1 % BSA. Total EphA2 and EphA2 phosphorylation were revealed utilizing a standard HRP format with a colorimetric reaction read at 450 nm by an ELISA Sunrise plate reader (Tecan, Männedorf, Switzerland). Data were normalized considering optical density (OD) of ephrin-A1-Fc alone as 100 % phosphorylation for pEphA2 and OD of unstimulated cells as 100 % for total EphA2.

2.5. 3-(4,5-Dimethylthiazol-2-yl)-2,5-diphenyltetrazolium bromide (MTT) assay

Antiproliferative and/or cytostatic capacity of the compounds was tested by using MTT assay at different time points: 24, 48 and 72 h. Briefly, 90 μL/well of $5x10^4$ cells/mL cells were seeded in 96 well Falcon® plates (Corning, Corning, NY, USA, #353072) and incubated for 24 h at 37 °C before the addition of test compounds for the required time. Prior to collection, MTT solution (1 mg/mL complete medium) was added and incubated for 2 h with the cells before assessment of MTT activity by absorbance using an ELISA Sunrise plate reader (Tecan, Männedorf, Switzerland) at wavelength of 550 nm.

2.6. Wound healing assay

Migration inhibition mediated by UniPR1449 was assessed in wound healing assays. U251 cells were seeded in 24-well Costar® plates (Corning, Corning, NY, USA, #3524) at a concentration of 7×10^4 cells/well in 750 μL/well of complete cell media and incubated at 37 °C until reaching a confluent monolayer. Then, a straight scratch was perforrmed across the monolayer using a sterile 1000 μL pipette tip. Cell media was aspirated and cells were rinsed with 1 mL/well of DPBS (Euroclone, Milan, Italy, #ECB4004L) to remove detached cells and debris. Next, 900 μL/well of serum-free medium were added. Subsequently, 100 μL/well of compound (UniPR1449 30 μM and 10 μM) 10× or control (3 % DMSO in PBS) were added. Images of the wound area were captured at time 0 (T_0) and after 24 h (T_{24}) using Leica DMi1 inverted microscope (Leica Camera, Wetzlar, Germany) at 2.5× magnification. Two fields/well were captured following previously drawn lines. The wound area was measured using ImageJ Java software. The percentage of wound closure was calculated according to the formula:

$$Wound\ closure(\%) = \frac{A_0 - A_t}{A_t} \times 100$$

where A_0 is the initial wound area and A_t is the area at time t.

Data were then normalised on control group migration.

2.7. Boyden chamber migration assay

3D Boyden chamber cell migration was evaluated using Falcon® permeable supports (Corning, Corning, NY, USA, #353097) with polycarbonate membranes and 8.0 μm pores. Briefly, U251 cells were seeded in the upper chamber at a concentration of $7.5x10^4$ cells/well in 270 μL/well of serum-free medium. The lower chamber of 24-well Falcon® plate (Corning, Corning, NY, USA, # 353504) was filled with 720 μL/well of complete medium to serve as chemoattractant. Next, 30 μL/well (upper chamber) and 80 μL/well (lower chamber) of UnPR1449 (30 μM and 10 μM) 10X or control (3 % DMSO in PBS) were added,

Following 24 h of incubation at 37 °C, non-migrated cells on the upper surface of the membrane were scraped off with cotton swabs and rinsed with 300 μL/well of PBS. Migrated cells were fixed with iced cold methanol and incubated for 10 min at 4 °C. Next, cells were stained with crystal violet (0.2 % in 25 % aqueous methanol) and incubated for 10 min at room temperature. Five washes with distilled water were performed to remove any excess of dye.

Dry membranes were imaged using Leica DMi1 inverted light microscope (Leica Camera, Wetzlar, Germany) at 4X magnification. Three randomly photographed fields per membrane were selected and cells were manually counted using ImageJ software.

2.8. In vitro immunocytochemistry

Internalization of EphA2 receptor: cells were fixed in 4 % paraformaldehyde (PFA), permeabilised in 0.5 % Triton X-100 and blocked in 10 % serum in PBS. Then, cells were incubated with primary antibody 15 μg/mL (Human EphA2 Antibody, R&D system, Minneapolis, MN, USA, #AF3035) overnight at 4 °C in PBS + 10 % serum. Secondary antibodies (Donkey anti-Goat 488, 1:1000, Thermo Fisher Scientific, Waltham, MA, USA, #SA5-10086) were diluted in 10 % serum in PBS and incubated at room temperature for 1 h. Coverslip were mounted with VECTASHIELD® Antifade Mounting Medium with DAPI (VectorLab, Newark, CA, USA, #H-1200–10) for 20 min. Imaging was carried out using the LEICA Stellaris 5 (Leica, Wetzlar, Germany). Images analysis was performed using Fiji ImageJ.

2.9. Stem cells characterization

The cell line utilized in this study is identical to that previously employed and thoroughly characterized by Brooks et al.[27]. Briefly, xenografts were performed using NOD-SCID-IL2R gamma chain-deficient (NSG) female mice at 8 weeks of age. Mice underwent stereotactic implantation of 1×10^5 GCGR-L11 cells (anteroposterior 0, mediolateral −2.5, dorsoventral −3.5) and were monitored for signs of disease when the mice were collected by transcardial perfusion with 4 % PFA under terminal anaesthesia. Brains were stored in 4 % PFA overnight before sectioning (50 μm) on a vibratome (Leica, Wetzlar, Germany, # VT1200S). For immunohistochemistry, sections were permeabilised in PBS, containing 1 % triton-x-100 and 10 % donkey serum, overnight at 4 °C and then incubated in primary antibodies (anti-

chicken GFP, 1:1000, #ab13970; mouse anti-nestin, 1:1000, #ab6142; rabbit anti-Sox2, 1:400, #ab97959, Abcam, Cambridge, UK) overnight at 4 °C. Sections were washed in PBS containing 0.1 % triton-x-100 before incubation in secondary antibodies (Donkey anti-chicken, Alexa Fluor™ 488, 1:1000, #A78948; Donkey anti-mouse, Alexa Fluor™ 647, 1:1000,#A-31571; Donkey anti-rabbit, Alexa Fluor™ 555, 1:1000, #A-31572, Thermo Fisher Scientific, Waltham, MA, USA) for 3 h in PBS containing 0.5 % triton-x-100 and 10 % donkey serum. Sections were washed and mounted on slides using prolong gold antifade mountant (P36934, ThermoFisher) followed by imaging on Zeiss LSM880 confocal microscope (Zeiss, Oberkochen, Germany).

2.10. Flow cytometry analysis

For proliferation studies, cells were treated with 5-ethynyl-2′-deoxyuridine (EdU) for 30 min before fixation and EdU stained using Click-iT™ EdU Alexa Fluor™ 488 Flow Cytometry Assay Kit (Thermo Fisher Scientific, Waltham, MA, USA, # C10420).

In brief, cells were fixed in 4 % PFA, permeabilised in 1 % Triton X-100 and blocked in 5 % BSA in PBS before incubation in Click-IT cocktail for 30 min at room temperature and staining with Dapi (1:10,000 in PBS containing 0.5 % Triton-X-100). Analysis of EdU incorporation was performed using BD Fortessa X20 (Becton Dickinson, Franklin Lakes, NJ, USA). Data analysis was performed using FlowJo software (Williamson Way, OR, USA).

2.11. Chick-embryo chorioallantoic membrane assay

The assay was performed as already described [22]. Briefly, a window was opened in the eggshell of three-day-old, fertilized chicken eggs (Azienda Agricola Crescenti s.r.l, Brescia, Italy). At day 11, alginate plugs containing VEGF-165 (R&D Systems, Minneapolis, MN, USA, #293-VE/CF) (1 µl, 4.5 pmoles/embryo) or FGF2 (R&D Systems, Minneapolis, MN, USA, #100-18B) (1 µl, 5,5 pmoles/embryo) in the absence or in the presence of the compound (2 µl, 20 pmoles/embryo) were placed on the CAMs (8 embryos per group). At day 14, newly formed blood microvessels converging toward the implant were analysed.

2.12. Statistical analysis

Data are the means of at least 3 independent experiments ± st.dev. One-way ANOVA followed by Tukey post-test was performed to compare 3 or more groups. Two tails, unpaired *t*-test was used to compare 2 groups. Charts, calculations and statistical analyses were performed on GraphPad Prism 9.5.1 (GraphPad Software Inc., La Jolla, CA, USA).

3. Results

3.1. EphA2 phosphorylation on U251 human GBM cells

The effect of compound UniPR1449 on EphA2 activity was tested in U251 human GBM cell line. Preliminary experiments demonstrated that incubation of U251 cells for 2 h with UniPR1449, at 10 and 30 µM, did not cause any non-specific toxic effects as determined by LDH quantification (Fig. 1A).

UniPR1449 was thus tested for its ability to interfere with EphA2 phosphorylation at the same concentrations. Briefly, EphA2-tyrosine phosphorylation was induced by incubation with 0.1 µg/ml ephrin-A1-Fc in the presence or absence of UniPR1449. The compound at 30 µM alone was unable to induce EphA2 phosphorylation whereas it reduced EphA2 phosphorylation when the receptor was stimulated with ephrin-A1-Fc (Fig. 1B). Dasatinib 300 nM completely abolished EphA2 phosphorylation induced by ephrin-A1-Fc.

3.2. EphA2 degradation and internalization

According to the literature, the cell membrane-expressed EphA2 receptor undergoes internalization and subsequent degradation upon stimulation by its ligand, ephrin-A1 [28]. Also in our hands, Ephrin-A1-Fc induces EphA2 receptor degradation in U251 cells. While EphA2 internalization was not blocked by dasatinib, the protein–protein interaction (PPI) antagonist UniPR1449 (at 30 µM and 10 µM) dose-dependely inhibited EphA2 degradation in presence of ephrin-A1-Fc (Fig. 2).

An immunofluorescent analysis was perfomed to confirm the antagonistic profile of UniPR1449, in response to ephrin-A1-Fc treatment. Cells were pretreated for 20 min with 0.3 % DMSO or UniPR1449 at 30 µM and 10 µM, followed by stimulation with ephrin-A1-Fc (0.1 µg/mL) for 2 h. Stimulation with ephrin-A1-Fc promoted EphA2 internalization, as evidenced by the accumulation of receptor-specific fluorescence within cells pretreated with vehicle. In contrast, pretreatment with UniPR1449 reduced receptor internalization in a concentration dependent manner, keeping EphA2 predominantly at the plasma

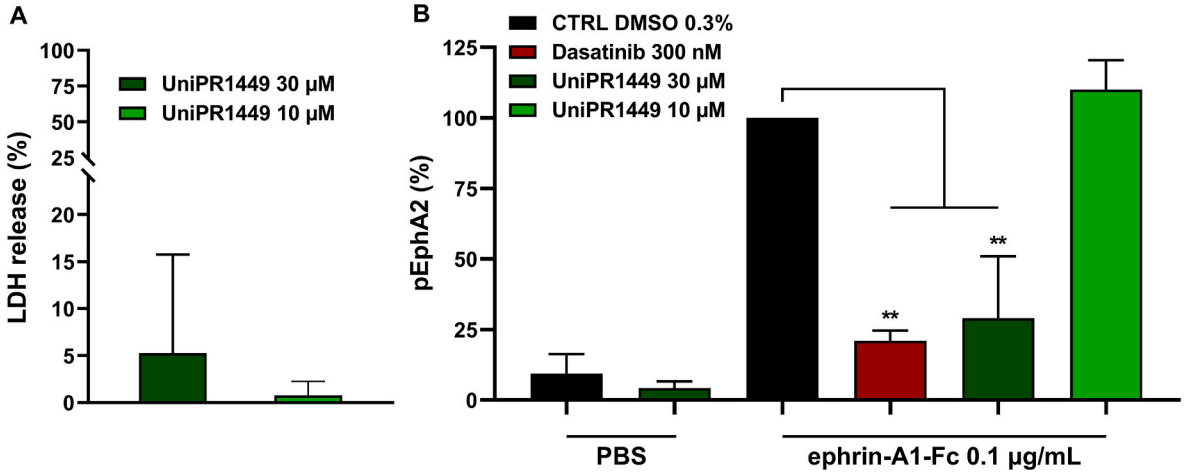

Fig. 1. **A** LDH release from human U251 GBM cells when incubated for two hours with UniPR1449. 0.3 % DMSO and Triton-X100, both not shown, were considered as 0 % and 100 % toxicity, respectively. **B** Phosphorylation of EphA2 in U251 cells. Cells were pretreated for 20 min with 0.3 % DMSO or with the compounds at the indicated concentrations and then stimulated for 10 min with ephrin-A1-Fc 0.1 µg/ml. Phospho-EphA2 levels are relative to DMSO 0.3 % + ephrin-A1-Fc. One-way ANOVA followed by Tukey's post-test was performed to compare DMSO 0.3 % + ephrin-A1-Fc to the columns of compound + ephrin-A1-Fc. **$p < 0.01$. Data are the means of at least 3 independent experiments ± st.dev.

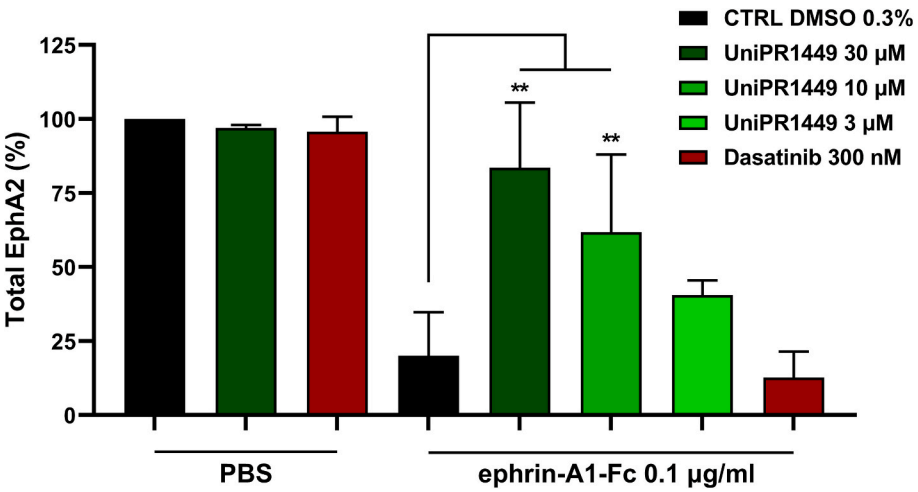

Fig. 2. Degradation of EphA2 in U251 cells. Cells were pretreated for 20 min with 0.3% DMSO or with the compounds at the indicated concentrations and then stimulated for 4 h with ephrin-A1-Fc 0.1 μg/mL or Fc alone. EphA2 levels are relative to the unstimulated condition (DMSO 0.3 % for 20 min + Fc for 4 h). One-way ANOVA followed by Tukey's post-test was performed to compare DMSO 0.3 % + ephrin-A1-Fc to all the other columns stimulated with ephrin-A1-Fc.**$p < 0.01$. Data are the means of at least 3 independent experiments ± st.dev.

membrane (Fig. 3).

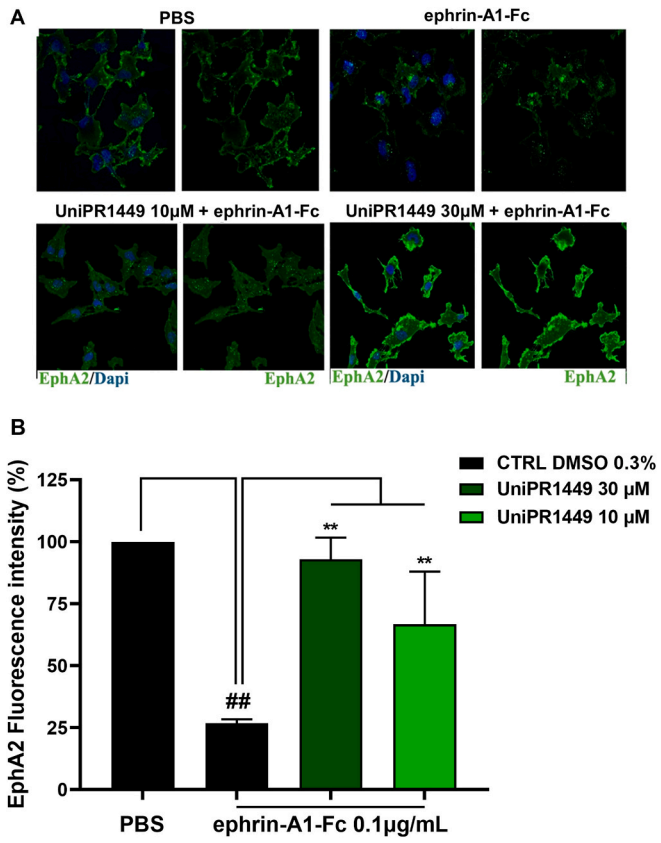

Fig. 3. Internalization of EphA2 in U251 cells. **A** Cells were pretreated for 20 min with 0.3 % DMSO or with UniPR1449 at the indicated concentrations and then stimulated for 2 h with ephrin-A1-Fc 0.1 μg/mL. Localization of receptor EphA2 was visualised by confocal microscopy. **B** Quantification of the images in A using ImageJ software. Results are corrected total cell fluorescence: integrated density − (area of selected cell × mean fluorescence of background). One-way ANOVA followed by Tukey's post-test was performed to compare DMSO 0.3 % + ephrin-A1-Fc to all the other columns stimulated with ephrin-A1-Fc.**$p < 0.01$. One-way ANOVA followed by Tukey's post-test was performed to compare DMSO 0.3 % + PBS to DMSO 0.3 % + ephrin-A1-Fc. ##$p < 0.01$. Data are the means of at least 3 independent experiments ± st.dev.

3.3. Effect of UniPR1449 on cell migration

U251 human GBM cells were treated with two different concentrations of the compound (10 μM and 30 μM) in a monolayer wound healing assay. Treatment with UniPR1449 at 30 μM significantly impaired migration compared to vehicle-traetment control whilst treatment with compound at 10 μM displayed a negligible activity (Fig. 4A). We next investigated the ability of UniPR1449 to modify the migratory phenotype of U251 cells by using a 3D Boyden chamber assay. UniPR1449 was able to reduce the amount of migrated cells of about 50 % at 30 μM compared to control cells (Fig. 4B). Representative images are reported in Fig. 4C.

Cell viability (MTT) and membrane integrity (LDH) assays were performed in parallel (data not shown). At 24 h of treatment no cytotoxicity was detected, although a reduction in metabolic activity, suggestive of a cytostatic effect, was observed. Thus, the decrease in migration is unlikely to be due to cell death, but rather reflects impaired motility or reduced metabolic activity.

3.4. Validation of GCGR L11 cell line

The GCS line GCGR L11 was selected as a model to investigate the activity of UniPR1449 on cell steamness. GCGR L11 overexpresses the EphA2 receptor in addition to EphA4, EphB3 and EphB4 (Fig. 5A), consistent with previous results [27], and resulted positive for two key stem cell markers, Sox2 and Nestin (Fig. 5B), with the first being a transcription factor associated with the maintenance of the undifferentiated state of cancer stem cells and the second a protein associated with self-renewal/proliferation and migration/invasion capability [29]. Taken together, these data supported the selection of the GCGR L11 cell line for further studies.

3.5. GSCs viability

Next, we evaluated the potential antiproliferative or cytostatic effects of UniPR1449, with the parental compound UniPR1331 as control. GCGR L11 cells were incubated with the compounds over different time periods (24, 48, and 72 h) and analyzed using the MTT assay. UniPR1449 10 μM showed a cytotoxic effect after 72 h of incubation, whereas lower concentrations (1 and 3 μM) exerted a cytostatic effect. The concentration reducing the 50 % proliferation was calculated as 2.4 μM for UniPR1449 (Fig. 6A). On the other hand, UniPR1331, used at the same concentrations, exhibited no effect (Fig. 6B).

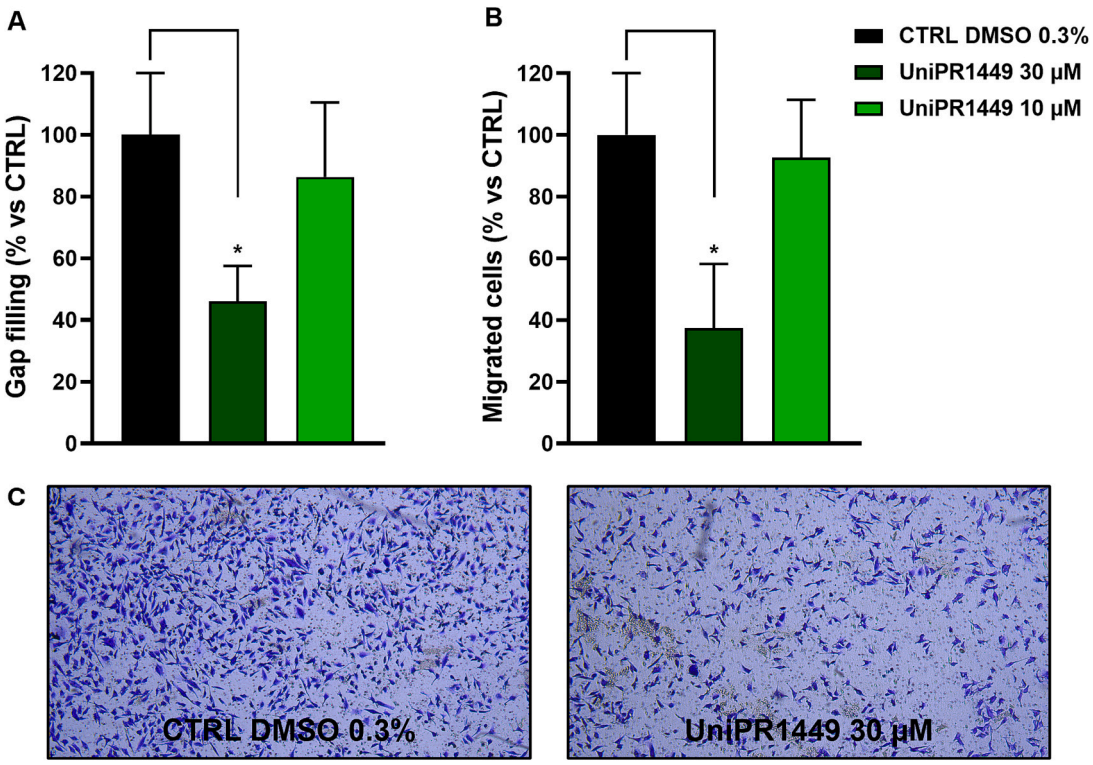

Fig. 4. Cell migration on U251 cells. **A** Wound scratching was performed on a confluent monolayer of cells using a P1000 sterile tip. Cells were cultured in serum-free medium for 24 h in presence of UniPR1449 (10 and 30 μM) or DMSO 0.3 %. Migration was assessed as reported in materials and methods. **B** Cells were cultured in Transwell Falcon® supports in a serum-free medium. The lower chamber was filled with complete medium using FBS as chemoattractant. UniPR1449 (10 and 30 μM) or DMSO 0.3% were added in both chambers immediately after seeding. Cells were incubated for 24 h and then non-migrated cells were removed with cotton swabs. Migrated cells were then fixed with methanol and stained with crystal violet dye and directly counted using ImageJ software. One-way ANOVA followed by Tukey's post-test was performed to compare vehicle-treated group vs compound treated group. *$p < 0,05$. Data are the means of at least 3 independent experiments ± st.dev. **C** Pictures of crystal violet stained cells on Falcon® permable membranes.

Given the limitations of the MTT assay for assessing GSCs metabolism and proliferation [30] we employed a flow cytometry-based approach namely, EdU incorporation assay to evaluate the anti-proliferative effects of UniPR1449 on GSCs to a better extent. Treatment with UniPR1449 for 72 h significantly reduced the proportion of cells in S-phase at both 10 μM and 3 μM concentrations (Fig. 7**A,B**). Given the inactivity of UniPR1331 in the MTT assay, it was excluded from further analysis.

3.6. Angiogenesis

In a previous study, we demonstrated the inhibitory effects of UniPR1331 on VEGF/VEGFR-2-driven neovascularization in the CAM model [22]. Thus, the same model was used here to evaluate the anti-angiogenic activity of UniPR1449. As shown in Fig. 8A, UniPR1449 did not alter the basal vascularization observed in the alginate plug containing vehicle alone, while it significantly inhibited VEGF-induced neovascularization. The specificity of the inhibitory effect exerted by UniPR1449 on the VEGF/VEGFR-2 axis was proven by the observation that, in the same experimental conditions, it did not inhibit neovascularization induced by a different angiogenic growth factor such as FGF2 (Fig. 8B).

4. Discussion

Significant efforts are currently being dedicated to the development of effective anticancer therapies, particularly for aggressive cancers such as gliomas. Extensive research on the VEGF/VEGFR2 system, aimed at starving the tumor through the inhibition of angiogenesis, culminated in the development of the anti-VEGF monoclonal antibody bevacizumab (Avastin, INN-bevacizumab) [31]. Unfortunately bevacizumab and other antiangiogenic drugs used as monotherapies in GBM have shown limited clinical success, increasing progression free survival but with no benefits on overall survival [32,33]. Bevacizumab is currently used in combination cancer treatment of many advanced or metastatic solid tumors including breast, renal, ovarian and non small cell lung cancers. Failure of antiangiogenic agents are likely due to the development of drug resistance, the redundant nature of the angiogenesis processes and the escaping contribution of GSCs [34].

To address this challenge, researchers have explored drug combinations that target different molecular pathways [35] or designed multitarget drugs capable of simultaneously blocking multiple therapeutic targets [36].

The dual targeting of VEGFR2 and Eph receptors may represent a promising strategy for treating GBM for multiple reasons:

i) there is a cross-talk between the VEGF/VEGFR2 and Eph/ephrin systems [37];
ii) they play roles in tumor cell proliferation, metastasis [3,38], and neovascularization [18];
iii) they are expressed in both cancer cells and endothelial cells (ECs);
iv) the VEGF/VEGFR2 [8,39,40] and Eph/ephrin systems are involved in regulating various aspects of GSCs phenotype, including proliferation, migration, and invasion. EphA2, EphA3 and EphB2 are overexpressed in GSCs, maintaining their stem-like properties and tumorigenicity [41].
v) preclinical studies showed that inhibiting the VEGF/VEGFR system depletes GSCs niches [40] and interfering with the Eph/ephrin signaling suppresses GSCs-driven tumor growth and

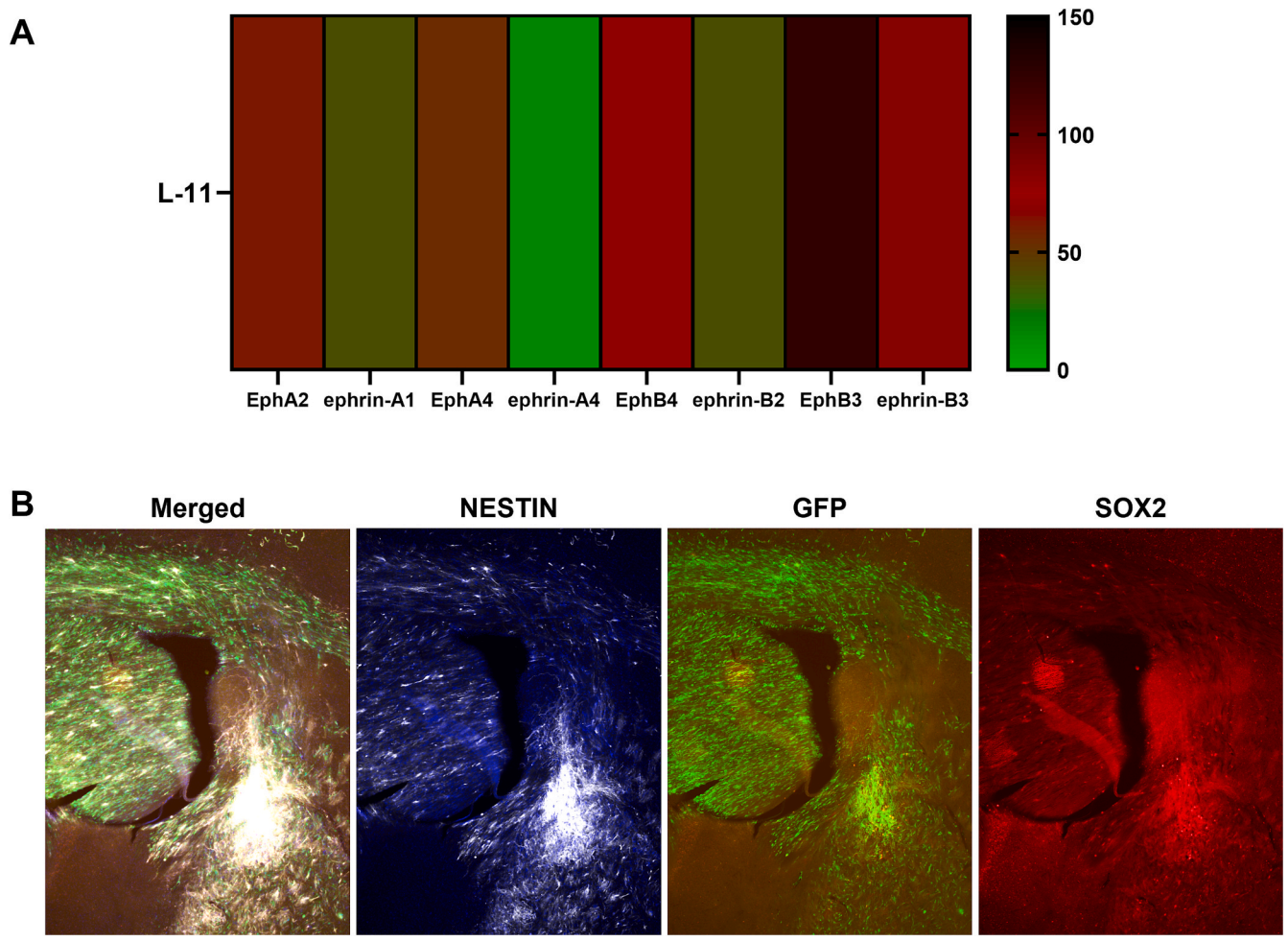

Fig. 5. **A** Heat map showing the levels of expression for some Eph receptors and their ligands in GCGR L11 cell line. **B** Images (20x) of mouse brain sections taken from a xenograft GCGR L11 injected mouse brain stained for nestin (grey) and Sox2 (red). Tumour cells are shown in green (GFP) and nuclei counterstained with Dapi (blue).

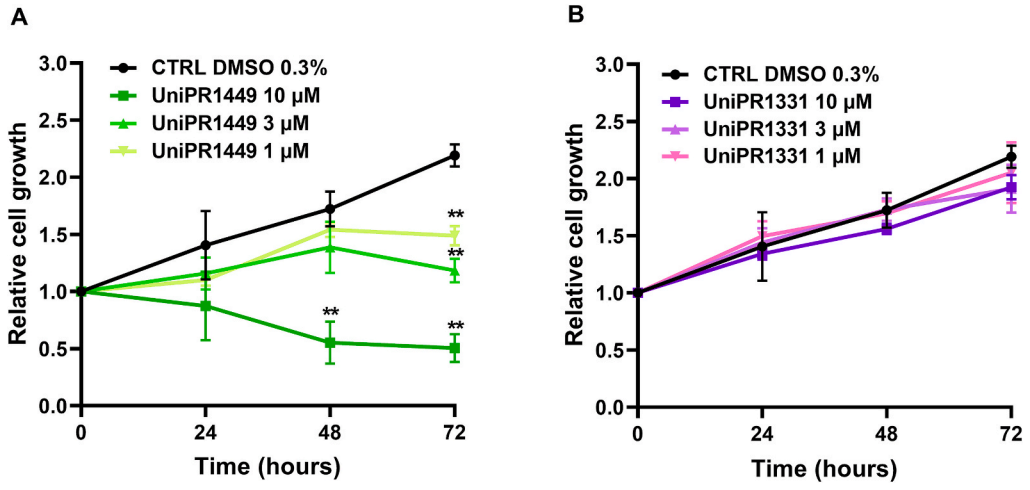

Fig. 6. Growth curves of GCGR L11 in the presence or absence of UniPR1449 (left) or UniPR1331 (right). Two-way ANOVA followed by Dunnet's post-test was performed to compare control curve to all the other curves. ** $p < 0.01$. Data are the means of at least 3 independent experiments ± st.dev.

enhances therapy efficacy [13]. Targeting Eph/ephrins could disrupt GSCs maintenance and reduce glioma aggressiveness [16].

Our findings demonstrate that UniPR1449 shows a panel of consistent effects of antagonist nature, inhibiting EphA2-ephrin-A1 interaction: 1- EphA2 phosphorylation reduction, 2- receptor internalization and degradation inhibition upon ephrin-A1-Fc stimulation and 3- no

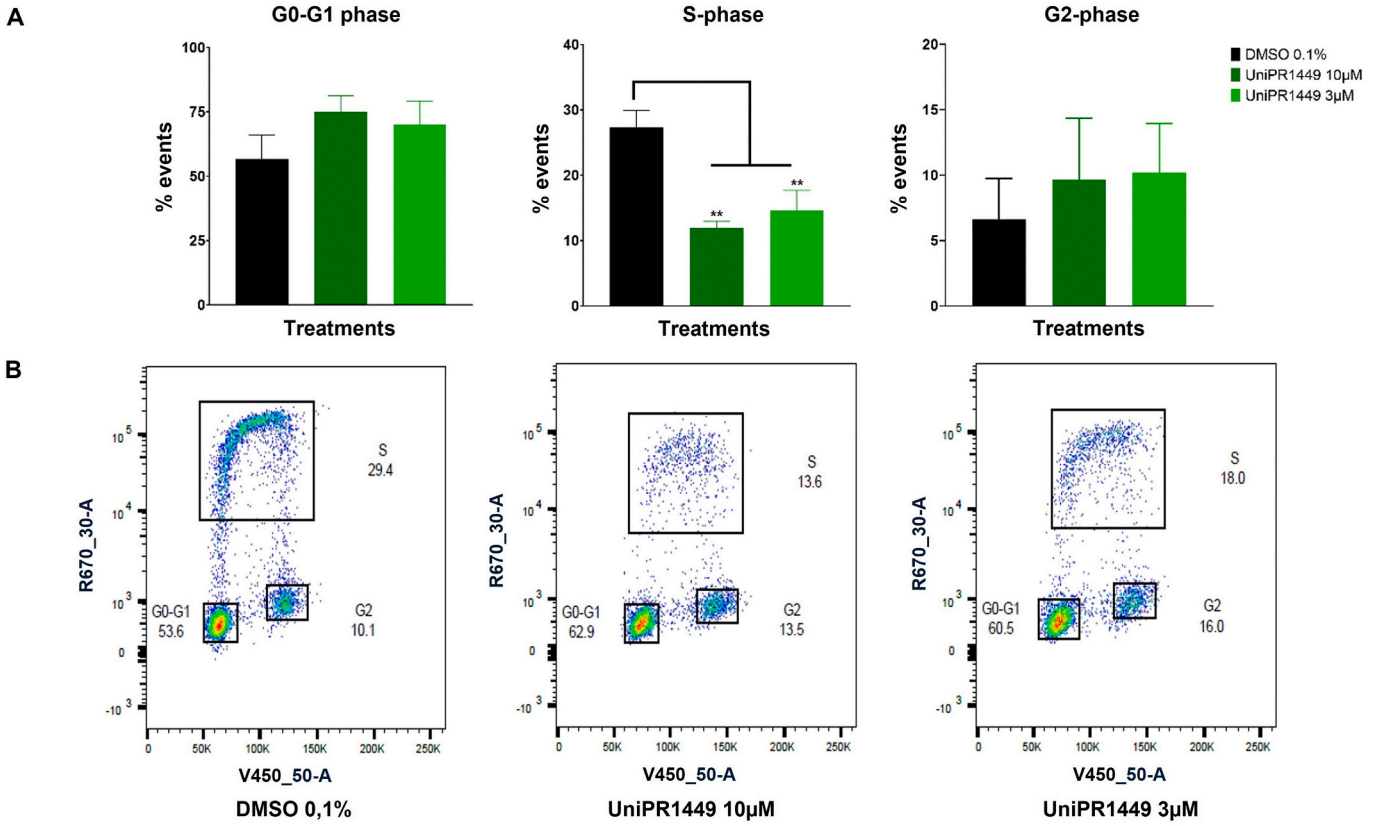

Fig. 7. **A** Quantification of cell cycle results in GCGR L11 cell line in presence of different concentrations of UniPR1449. The assay was conducted at 24, 48 (data not shown) and 72 h. **B** The dot plots show the corresponding flow cytometry fluorescence intensity distributions (R670_30-A vs V450_50-A), with gated populations indicating cells in G0-G1, S, and G2 phases. One-way ANOVA followed by Tukey's post-test was performed to compare control curve to all the other curves. **p < 0.01. Data are the means of at least 3 independent experiments ± st.dev.

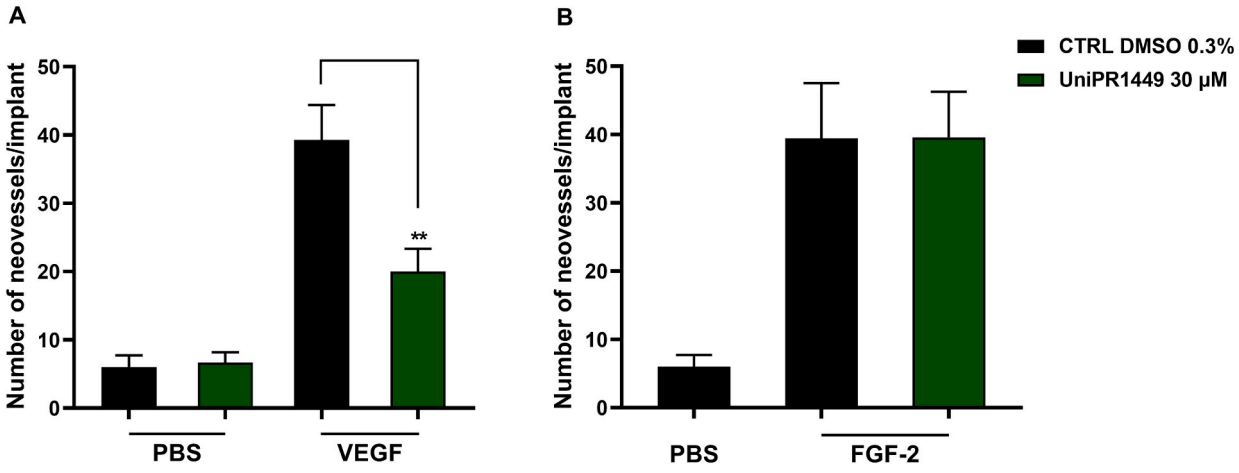

Fig. 8. **A** Number of vessels in CAM model in presence of VEGF and compounds with or without VEGF. **B** Graph reporting the number of vessels in CAM model in presence of FGF2 and compounds with FGF2. One-way ANOVA followed by Tukey's post-test was performed to compare DMSO + VEGF/FGF to UniPR1449 + VEGF/FGF (**p < 0.01). Data are the means of at least 3 independent experiments ± st.dev.

activation of EphA2 on its own. Similarly, the kinase inhibitor dasatinib strongly inhibited EphA2 phosphorylation. On the other hand, dasatinib did not prevent EphA2 degradation in the presence of ephrin-A1-Fc. Similar data have been reported by Q. Chang where dasatinib was almost ineffective in inhibiting EphA2 degradation upon ephrin-A1 stimulation on MIA PaCa-2 and PANC-1 pancreatic cancer cell lines [42].

A recent study highlights that EphA2 activation by ephrin-A2 can promote a migratory behavior of GBM cells, whilst ephrin-A1 binding is extensively reported as inhibitor of this oncogenic effect [43]. In addition, other data indicate that tumor cells can cleave membrane-bound ephrins, thereby releasing soluble monomeric proteins with functional activity in the cell medium [44]. Such heterogeneity confuses the interpretation of ligand-specific effects on migration. To address this issue, we assessed cell migration in the absence of exogenous ephrin stimulation. Our data shows that UniPR1449 reduces cell motility,

suggesting its potential activity on a broader spectrum of EphA2 natural ligands, and conceivably impairing cancer cells dissemination.

We had previously reported that the Eph-ephrin antagonism may be a valid strategy to tackle GBM as demonstrated by the activity of the pan Eph-ephrin interaction inhibitor UniPR1331 in a murine model of GBM [21]. Similarly to UniPR1331 [22], UniPR1449 exhibited anti-angiogenic activity in our CAM model, likely due both to the cross-talk between VEGFR2 and the ephrin system and to the direct inhibition of VEGFR2 activity. The lack of activity against FGFR2-mediated angiogenesis, supports that the antiangiogenic effect displayed by UniPR1449 is specific and not driven by non-specific cytotoxic events.

Considering the role of GSCs in tumor persistence and resistance to therapy, we investigated the effects of UniPR1449 in the GCGR L11 GSC line. MTT assays revealed that UniPR1449 displayed both cytostatic and cytotoxic effects in a dose-dependent manner. Notably, UniPR1331, the parent compound, showed no significant activity. Given the limitations of the MTT assay in GSCs, we utilized an EdU incorporation assay to directly assess DNA synthesis. Results suggest a significant reduction in the S-phase population, reinforcing the antiproliferative effects of this compound.

The differential inhibitory profiles of UniPR1449, an EphA-ephrin-As-inhibitor, in comparison to the parent compound UniPR1331, a pan Ephs-ephrins-inhibitor, provide novel insights into the ephrin system's role in GBM. Indeed, our data are in agreement with prior studies suggesting that Eph-ephrin-A system is essential for maintaining GBM stemness [13,16,45].

Overall, our study underscores the potential of UniPR1449 as an innovative pharmacological tool in GBM by targeting both tumor proliferation and angiogenesis. These findings justify further *in vivo* investigations to explore its efficacy and therapeutic applicability, paving the way for novel treatment strategies in GBM management. In this view, selective EphA antagonism may offer a safer profile compared to pan-Eph inhibitors such as UniPR1331 by sparing EphB-mediated physiological functions. In central nervous system Eph-ephrin-Bs system was demonstrated to be a key player in regulating sinapse density in cortical neurons [46]. In the intestine, EphB2/B3 maintain crypt architecture and barrier integrity and their inhibition may risk colitis and tumorigenesis [47,48]. In cardiovascular/neural systems, EphB4/B2 regulate physiological angiogenesis and neurovascular coupling and a pan-Eph blockade may trigger thrombosis and/or synaptic dysfunction [49,50]. Selective targeting of EphAs overexpressed in GBM including GSCs, could minimize gut-, vascular-, and neuro-toxicity, enhancing therapeutic window.

5. Funding sources

This work was supported by Associazione Italiana Ricerca sul Cancro (AIRC IG 22873) to MT. The funder had no role in study design, data collection and analysis, decision to publish, or preparation of manuscript. This work has been carried out in the frame of the ALIFAR project, funded by the Italian Ministry of University through the program "Dipartimenti di Eccellenza 2023–2027". MC was supported by PNRR – CN3 "Sviluppo di Terapia Genica e Farmaci con Tecnologia ad RNA" funded by NextGenerationEU.

Declaration of Generative AI and AI-assisted technologies in the writing process

During the preparation of this work the authors used AI in order to improve the readability of some sentences. After using this service, the authors reviewed and edited the content as needed and takes full responsibility for the content of the publication.

CRediT authorship contribution statement

Alfonso Zappia: Writing – original draft, Methodology, Investigation, Data curation. **Francesca Romana Ferrari:** Validation, Investigation, Formal analysis, Data curation. **Carmine Giorgio:** Writing – review & editing, Visualization, Validation, Conceptualization. **Stefano Sala:** Investigation, Data curation. **Ilaria Zanotti:** Writing – review & editing. **Simona Parrinello:** Supervision, Resources. **Melanie P. Clements:** Methodology, Investigation. **Marco Rusnati:** Writing – review & editing, Resources. **Michela Corsini:** Investigation. **Andrea Blesio:** Data curation, Investigation, Writing – review & editing. **Riccardo Castelli:** Validation, Investigation. **Lorenzo Guidetti:** Investigation. **Laura Scalvini:** Software, Methodology. **Alessio Lodola:** Writing – review & editing, Supervision, Resources, Methodology. **Massimiliano Tognolini:** Writing – review & editing, Supervision, Resources, Project administration, Funding acquisition, Conceptualization.

Declaration of competing interest

The authors declare that they have no known competing financial interests or personal relationships that could have appeared to influence the work reported in this paper.

Acknowledgements

Dr. Bonati Rosaria is kindly acknowledged for her technical support.

Data availability

Data will be made available on request.

References

[1] H. Hirai, Y. Maru, K. Hagiwara, J. Nishida, F. Takaku, A novel putative tyrosine kinase receptor encoded by the eph gene, Science 238 (1987) 1717–1720.
[2] L.-Y. Liang, O. Patel, P.W. Janes, J.M. Murphy, I.S. Lucet, Eph receptor signalling: from catalytic to non-catalytic functions, Oncogene 38 (2019) 6567–6584, https://doi.org/10.1038/s41388-019-0931-2.
[3] E.B. Pasquale, Eph receptors and ephrins in cancer progression, Nat. Rev. Cancer 24 (2024) 5–27, https://doi.org/10.1038/s41568-023-00634-x.
[4] D.A. Kirschmann, E.A. Seftor, K.M. Hardy, R.E.B. Seftor, M.J.C. Hendrix, Molecular pathways: vasculogenic mimicry in tumor cells: diagnostic and therapeutic implications, Clin. Cancer Res. 18 (2012) 2726–2732, https://doi.org/10.1158/1078-0432.CCR-11-3237.
[5] H. Miao, D.-Q. Li, A. Mukherjee, H. Guo, A. Petty, J. Cutter, J.P. Basilion, J. Sedor, J. Wu, D. Danielpour, A.E. Sloan, M.L. Cohen, B. Wang, EphA2 mediates ligand-dependent inhibition and ligand-independent promotion of cell migration and invasion via a reciprocal regulatory loop with Akt, Cancer Cell 16 (2009) 9–20, https://doi.org/10.1016/j.ccr.2009.04.009.
[6] B.W. Day, B.W. Stringer, F. Al-Ejeh, M.J. Ting, J. Wilson, K.S. Ensbey, P. R. Jamieson, Z.C. Bruce, Y.C. Lim, C. Offenhäuser, S. Charmsaz, L.T. Cooper, J. K. Ellacott, A. Harding, L. Leveque, P. Inglis, S. Allan, D.G. Walker, M. Lackmann, G. Osborne, K.K. Khanna, B.A. Reynolds, J.D. Lickliter, A.W. Boyd, EphA3 maintains tumorigenicity and is a therapeutic target in glioblastoma multiforme, Cancer Cell 23 (2013) 238–248, https://doi.org/10.1016/j.ccr.2013.01.007.
[7] Y. Tu, S. He, J. Fu, G. Li, R. Xu, H. Lu, J. Deng, Expression of EphrinB2 and EphB4 in glioma tissues correlated to the progression of glioma and the prognosis of glioblastoma patients, Clin. Transl. Oncol. 14 (2012) 214–220, https://doi.org/10.1007/s12094-012-0786-2.
[8] N. Jhaveri, T.C. Chen, F.M. Hofman, Tumor vasculature and glioma stem cells: Contributions to glioma progression, Cancer Lett. 380 (2016) 545–551, https://doi.org/10.1016/j.canlet.2014.12.028.
[9] R. Stupp, W.P. Mason, M.J. Van Den Bent, M. Weller, B. Fisher, M.J.B. Taphoorn, K. Belanger, A.A. Brandes, C. Marosi, U. Bogdahn, J. Curschmann, R.C. Janzer, S. K. Ludwin, T. Gorlia, A. Allgeier, D. Lacombe, J.G. Cairncross, E. Eisenhauer, R. O. Mirimanoff, Radiotherapy plus concomitant and adjuvant temozolomide for glioblastoma, N. Engl. J. Med. 352 (2005) 987–996, https://doi.org/10.1056/NEJMoa043330.
[10] D. Krex, B. Klink, C. Hartmann, A. Von Deimling, T. Pietsch, M. Simon, M. Sabel, J. P. Steinbach, O. Heese, G. Reifenberger, M. Weller, G. Schackert, for the German Glioma Network, long-term survival with glioblastoma multiforme, Brain 130 (2007) 2596–2606, https://doi.org/10.1093/brain/awm204.
[11] L. Persano, E. Rampazzo, G. Basso, G. Viola, Glioblastoma cancer stem cells: Role of the microenvironment and therapeutic targeting, Biochem. Pharmacol. 85 (2013) 612–622, https://doi.org/10.1016/j.bcp.2012.10.001.
[12] A. Thakur, C. Faujdar, R. Sharma, S. Sharma, B. Malik, K. Nepali, J.P. Liou, Glioblastoma: current status, emerging targets, and recent advances, J. Med. Chem. 65 (2022) 8596–8685, https://doi.org/10.1021/acs.jmedchem.1c01946.

[13] E. Binda, A. Visioli, F. Giani, G. Lamorte, M. Copetti, K.L. Pitter, J.T. Huse, L. Cajola, N. Zanetti, F. DiMeco, L. De Filippis, A. Mangiola, G. Maira, C. Anile, P. De Bonis, B.A. Reynolds, E.B. Pasquale, A.L. Vescovi, The EphA2 receptor drives self-renewal and tumorigenicity in stem-like tumor-propagating cells from human glioblastomas, Cancer Cell 22 (2012) 765–780, https://doi.org/10.1016/j.ccr.2012.11.005.

[14] N. Trivieri, A. Visioli, G. Mencarelli, M.G. Cariglia, L. Marongiu, R. Pracella, F. Giani, A.A. Soriano, C. Barile, L. Cajola, M. Copetti, O. Palumbo, F. Legnani, F. DiMeco, L. Gorgoglione, A.L. Vescovi, E. Binda, Growth factor independence underpins a paroxysmal, aggressive Wnt5aHigh/EphA2Low phenotype in glioblastoma stem cells, conducive to experimental combinatorial therapy, J. Exp. Clin. Cancer Res. 41 (2022) 139, https://doi.org/10.1186/s13046-022-02333-1.

[15] H. Miao, N.W. Gale, H. Guo, J. Qian, A. Petty, J. Kaspar, A.J. Murphy, D. M. Valenzuela, G. Yancopoulos, D. Hambardzumyan, J.D. Lathia, J.N. Rich, J. Lee, B. Wang, EphA2 promotes infiltrative invasion of glioma stem cells in vivo through cross-talk with Akt and regulates stem cell properties, Oncogene 34 (2015) 558–567, https://doi.org/10.1038/onc.2013.590.

[16] M.A. Qazi, P. Vora, C. Venugopal, J. Adams, M. Singh, A. Hu, M. Gorelik, M. K. Subapanditha, N. Savage, J. Yang, C. Chokshi, M. London, A. Gont, D. Bobrowski, N. Grinshtein, K.R. Brown, N.K. Murty, J. Nilvebrant, D. Kaplan, J. Moffat, S. Sidhu, S.K. Singh, Cotargeting ephrin receptor tyrosine kinases A2 and A3 in cancer stem cells reduces growth of recurrent glioblastoma, Cancer Res. 78 (2018) 5023–5037, https://doi.org/10.1158/0008-5472.CAN-18-0267.

[17] B. Krusche, C. Ottone, M.P. Clements, E.R. Johnstone, K. Goetsch, H. Lieven, S. G. Mota, P. Singh, S. Khadayate, A. Ashraf, T. Davies, S.M. Pollard, P. De, F. Roncaroli, J. Martinez-Torrecuadrada, P. Bertone, S. Parrinello, EphrinB2 drives perivascular invasion and proliferation of glioblastoma stem-like cells, eLife 5 (2016), https://doi.org/10.7554/eLife.14845.001.

[18] W.N.A. Baharuddin, A.A.M. Yusoff, J.M. Abdullah, Z.F. Osman, F. Ahmad, Roles of EphA2 receptor in angiogenesis signaling pathway of glioblastoma multiforme, Malays, J. Med. Sci. 25 (2018) 22–27, https://doi.org/10.21315/mjms2018.25.6.3.

[19] M. Tognolini, F.R. Ferrari, A. Zappia, C. Giorgio, Ephrin receptor type-A2 (EphA2) targeting in cancer: a patent review (2018-present), Expert Opin. Ther. Pat. 34 (2024) 1009–1018, https://doi.org/10.1080/13543776.2024.2402382.

[20] L. Guidetti, R. Castelli, L. Scalvini, F. Ferlenghi, M. Corrado, C. Giorgio, M. Tognolini, A. Lodola, Protein-protein interaction inhibitors targeting the eph-ephrin system with a focus on amino acid conjugates of bile acids, Pharmaceuticals (Basel) 15 (2022) 137, https://doi.org/10.3390/ph15020137.

[21] C. Festuccia, G.L. Gravina, C. Giorgio, A. Mancini, C. Pellegrini, A. Colapietro, S. Delle Monache, M.G. Maturo, R. Sferra, P. Chiodelli, M. Rusnati, A. Cantoni, R. Castelli, F. Vacondio, A. Lodola, M. Tognolini, UniPR1331, a small molecule targeting Eph/ephrin interaction, prolongs survival in glioblastoma and potentiates the effect of antiangiogenic therapy in mice, Oncotarget 9 (2018) 24347–24363, https://doi.org/10.18632/oncotarget.25272.

[22] M. Rusnati, G. Paiardi, C. Tobia, C. Urbinati, A. Lodola, P. D'Ursi, M. Corrado, R. Castelli, R.C. Wade, M. Tognolini, P. Chiodelli, Cholenic acid derivative UniPR1331 impairs tumor angiogenesis via blockade of VEGF/VEGFR2 in addition to Eph/ephrin, Cancer Gene Ther. 29 (2022) 908–917, https://doi.org/10.1038/s41417-021-00379-5.

[23] F. Ferlenghi, R. Castelli, L. Scalvini, C. Giorgio, M. Corrado, M. Tognolini, M. Mor, A. Lodola, F. Vacondio, Drug-gut microbiota metabolic interactions: the case of UniPR1331, selective antagonist of the Eph-ephrin system, in mice, J. Pharm. Biomed. Anal. 180 (2020) 113067, https://doi.org/10.1016/j.jpba.2019.113067.

[24] L. Guidetti, A. Zappia, L. Scalvini, F.R. Ferrari, C. Giorgio, R. Castelli, F. Galvani, F. Vacondio, S. Rivara, M. Mor, C. Urbinati, M. Rusnati, M. Tognolini, A. Lodola, Molecular determinants of EphA2 and EphB2 antagonism enable the design of ligands with improved selectivity, J. Chem. Inf. Model. 63 (2023) 6900–6911, https://doi.org/10.1021/acs.jcim.3c01064.

[25] L. Guidetti, R. Castelli, A. Zappia, F.R. Ferrari, C. Giorgio, E. Barocelli, L. Pagliaro, F. Vento, G. Roti, L. Scalvini, F. Vacondio, S. Rivara, M. Mor, A. Lodola, M. Tognolini, Discovery of a new 1-(phenylsulfonyl)-1H-indole derivative targeting the EphA2 receptor with antiproliferative activity on U251 glioblastoma cell line, Eur. J. Med. Chem. 276 (2024) 116681, https://doi.org/10.1016/j.ejmech.2024.116681.

[26] J. Wykosky, D.M. Gibo, C. Stanton, W. Debinski, EphA2 as a novel molecular marker and target in glioblastoma multiforme, Mol. Cancer Res. 3 (2005) 541–551, https://doi.org/10.1158/1541-7786.MCR-05-0056.

[27] L.J. Brooks, M.P. Clements, J.J. Burden, D. Kocher, L. Richards, S.C. Devesa, L. Zakka, M. Woodberry, M. Ellis, Z. Jaunmuktane, S. Brandner, G. Morrison, S. M. Pollard, P.B. Dirks, S. Marguerat, S. Parrinello, The white matter is a pro-differentiative niche for glioblastoma, Nat. Commun. 12 (2021) 2184, https://doi.org/10.1038/s41467-021-22225-w.

[28] J. Walker-Daniels, D.J. Riese, M.S. Kinch, c-Cbl-dependent EphA2 protein degradation is induced by ligand binding, Mol. Cancer Res. 1 (2002) 79–87.

[29] H.D. Hemmati, I. Nakano, J.A. Lazareff, M. Masterman-Smith, D.H. Geschwind, M. Bronner-Fraser, H.I. Kornblum, Cancerous stem cells can arise from pediatric brain tumors, Proc. Natl. Acad. Sci. U.S.A. 100 (2003) 15178–15183, https://doi.org/10.1073/pnas.2036535100.

[30] P.W. Sylvester, Optimization of the tetrazolium dye (MTT) colorimetric assay for cellular growth and viability, in: S.D. Satyanarayanajois (Ed.), Drug Design and Discovery, Humana Press, Totowa, NJ, 2011, pp. 157–168, https://doi.org/10.1007/978-1-61779-012-6_9.

[31] N. Ferrara, K.J. Hillan, H.-P. Gerber, W. Novotny, Discovery and development of bevacizumab, an anti-VEGF antibody for treating cancer, Nat. Rev. Drug Discov. 3 (2004) 391–400, https://doi.org/10.1038/nrd1381.

[32] A. Motamed-Sanaye, A. Mortezaei, A.R. Afshari, Z. Saadatian, A.H. Faraji, J. P. Sheehan, A.M. Mokhtari, Angiogenesis inhibitors effects on overall survival and progression-free survival in newly diagnosed primary glioblastoma multiforme: a meta-analysis of twelve randomized clinical trials, J. Neurooncol 171 (2025) 313–328, https://doi.org/10.1007/s11060-024-04865-2.

[33] C. Wang, L. Duan, Y. Zhao, Y. Wang, Y. Li, Efficacy and safety of bevacizumab combined with temozolomide in the treatment of glioma: a systematic review and meta-analysis of clinical trials, World Neurosurg. 193 (2025) 447–460, https://doi.org/10.1016/j.wneu.2024.10.071.

[34] M. Safari, A. Khoshnevisan, Cancer stem cells and chemoresistance in glioblastoma multiform: a review article, J. Stem Cells 10 (2015) 271–285.

[35] H. Su, Y. Peng, Y. Wu, X. Zeng, Overcoming immune evasion with innovative multi-target approaches for glioblastoma, Front. Immunol. 16 (2025) 1541467, https://doi.org/10.3389/fimmu.2025.1541467.

[36] J.-R. Wei, M.-Y. Lu, T.-H. Wei, J.S. Fleishman, H. Yu, X.-L. Chen, X.-T. Kong, S.-L. Sun, N.-G. Li, Y. Yang, H.-W. Ni, Overcoming cancer therapy resistance: from drug innovation to therapeutics, Drug Resist. Updat. 81 (2025) 101229, https://doi.org/10.1016/j.drup.2025.101229.

[37] S. Sawamiphak, S. Seidel, C.L. Essmann, G.A. Wilkinson, M.E. Pitulescu, T. Acker, A. Acker-Palmer, Ephrin-B2 regulates VEGFR2 function in developmental and tumour angiogenesis, Nature 465 (2010) 487–491, https://doi.org/10.1038/nature08995.

[38] J.-C. Chen, Y.-W. Chang, C.-C. Hong, Y.-H. Yu, J.-L. Su, The role of the VEGF-C/VEGFRs axis in tumor progression and therapy, Int. J. Mol. Sci. 14 (2012) 88–107, https://doi.org/10.3390/ijms14010088.

[39] E. Codrici, A.-M. Enciu, I.-D. Popescu, S. Mihai, C. Tanase, Glioma stem cells and their microenvironments: providers of challenging therapeutic targets, Stem Cells Int. 2016 (2016) 5728438, https://doi.org/10.1155/2016/5728438.

[40] R. Tamura, T. Tanaka, K. Miyake, K. Yoshida, H. Sasaki, Bevacizumab for malignant gliomas: current indications, mechanisms of action and resistance, and markers of response, Brain Tumor Pathol. 34 (2017) 62–77, https://doi.org/10.1007/s10014-017-0284-x.

[41] E.B. Pasquale, Eph receptors and ephrins in cancer: bidirectional signalling and beyond, Nat. Rev. Cancer 10 (2010) 165–180, https://doi.org/10.1038/nrc2806.

[42] Q. Chang, C. Jorgensen, T. Pawson, D.W. Hedley, Effects of dasatinib on EphA2 receptor tyrosine kinase activity and downstream signalling in pancreatic cancer, Br. J. Cancer 99 (2008) 1074–1082, https://doi.org/10.1038/sj.bjc.6604676.

[43] N. Hirai, S. Tamai, T. Ichinose, H. Sabit, N. Saito, S. Iwabuchi, M. Nakada, EphrinA2 promotes glioma cell migration and invasion through EphA2 and FAK, Cancer Cell Int. 25 (2025) 191, https://doi.org/10.1186/s12935-025-03826-7.

[44] J. Wykosky, E. Palma, D.M. Gibo, S. Ringler, C.P. Turner, W. Debinski, Soluble monomeric EphrinA1 is released from tumor cells and is a functional ligand for the EphA2 receptor, Oncogene 27 (2008) 7260–7273, https://doi.org/10.1038/onc.2008.328.

[45] P. Martins, R.C.J. D'Souza, N. Skarne, L. Lekieffre, S. Horsefield, M. Ranjankumar, X. Li, T.T. Le, F. Smith, C. Smith, J. Burrows, B.W. Day, R. Khanna, EphA3 CAR T cells are effective against glioblastoma in preclinical models, J. Immunother. Cancer 12 (2024) e009403, https://doi.org/10.1136/jitc-2024-009403.

[46] N.T. Henderson, S.J. Le Marchand, M. Hruska, S. Hippenmeyer, L. Luo, M.B. Dalva, Ephrin-B3 controls excitatory synapse density through cell-cell competition for EphBs, Elife 8 (2019) e41563, https://doi.org/10.7554/eLife.41563.

[47] P.V. Senior, B.X. Zhang, S.T.F. Chan, Loss of cell-surface receptor EphB2 is important for the growth, migration, and invasiveness of a colon cancer cell line, Int. J. Colorectal Dis. 25 (2010) 687–694, https://doi.org/10.1007/s00384-010-0916-7.

[48] Y. Chen, C. Huang, F. Du, Z. Xiao, W. Qian, T. Bai, J. Song, Y. Song, X. Hou, L. Zhang, EphB2 promotes enteric nitrergic hyperinnervation and neurogenic inflammation in DSS-induced chronic colitis in mice, Int. Immunopharmacol. 129 (2024) 111591, https://doi.org/10.1016/j.intimp.2024.111591.

[49] G. Luxán, J. Stewen, N. Díaz, K. Kato, S.K. Maney, A. Aravamudhan, F. Berkenfeld, N. Nagelmann, H.C. Drexler, D. Zeuschner, C. Faber, H. Schillers, S. Hermann, J. Wiseman, J.M. Vaquerizas, M.E. Pitulescu, R.H. Adams, Endothelial EphB4 maintains vascular integrity and transport function in adult heart, Elife 8 (2019) e45863, https://doi.org/10.7554/eLife.45863.

[50] Y. Wang, Z. Wu, H. Luo, J. Peng, J. Raelson, G.B. Ehret, P.B. Munroe, E. Stoyanova, Z. Qin, G. Cloutier, W.E. Bradley, T. Wu, J.-Z. Shen, S. Hu, J. Wu, The role of GRIP1 and ephrin B3 in blood pressure control and vascular smooth muscle cell contractility, Sci. Rep. 6 (2016) 38976, https://doi.org/10.1038/srep38976.